Oxygen abundances in the NLRs of Seyfert galaxies and the metallicity-luminosity relation

Mark Armah
Universidade Federal do Rio Grande do Sul (UFRGS)

Advisor : Prof. Rogério Riffel (UFRGS)

Collaborators:

O. L. Dors	Universidade do Vale do Paraíba
The BASS team:	Kyuseok Oh, Michael J. Koss, Claudio Ricci, Benny Trakhtenbrot
Mabel Valerdi	Instituto Nacional de Astrofísica, Óptica y Electrónica (INAOE)
Rogemar A. Riffel	Universidade Federal de Santa Maria
Angela C. Krabbe	Universidade do Vale do Paraíba

Mark Armah acknowledges support from the Fermi Summer School 2023 Organizers and the Center for Research and Exploration in Space Science and Technology II (CRESST II) agreement (80GSFC21M0002).

Why study the chemical composition of AGN hots?

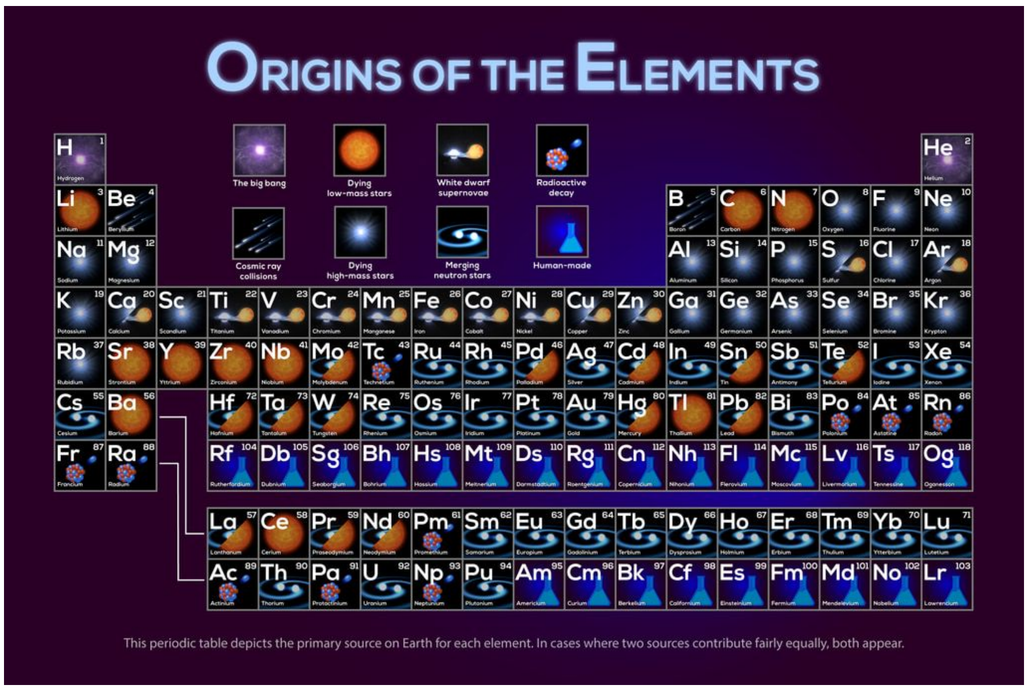

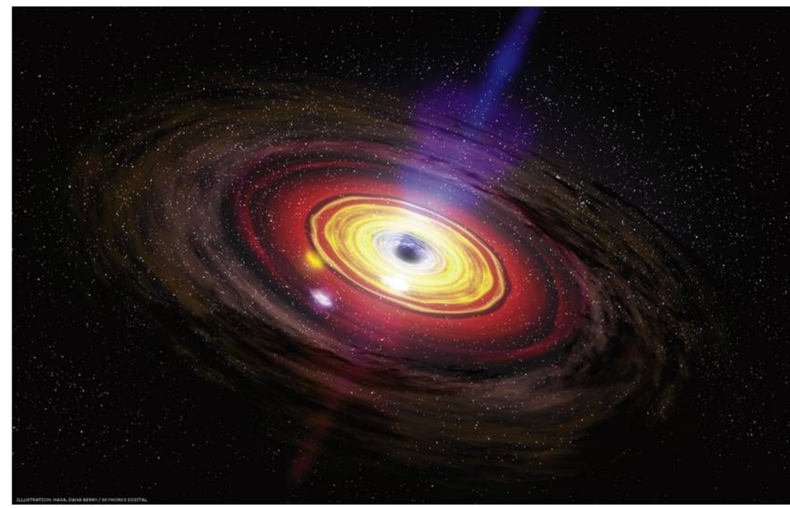

Metallicity and ISM Conditions

- Gas-phase and stellar metallicities show clear scaling relations with several integrated properties of galaxies

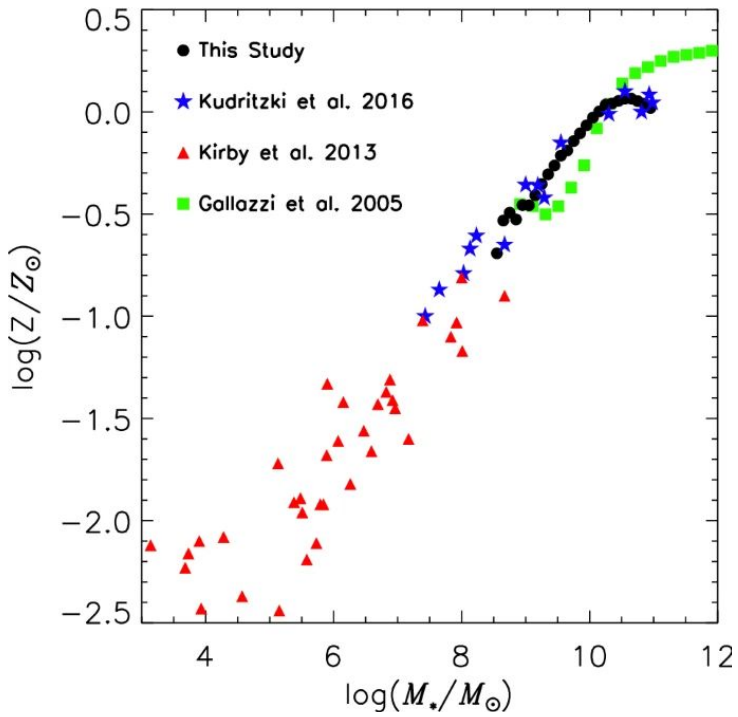

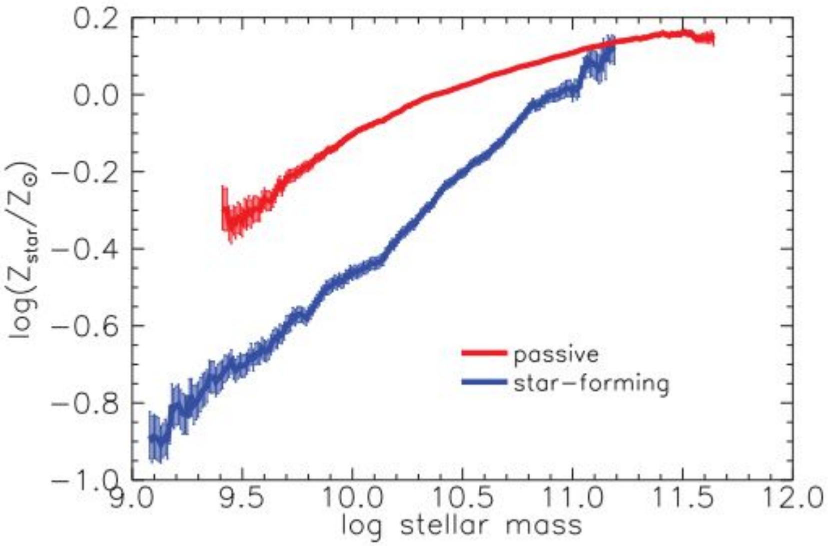

Maiolino & Mannucci, 2019 *Astron Astrophys Rev* **27**, 3

The mass-metallicity relation (MZR) controversy in AGNs

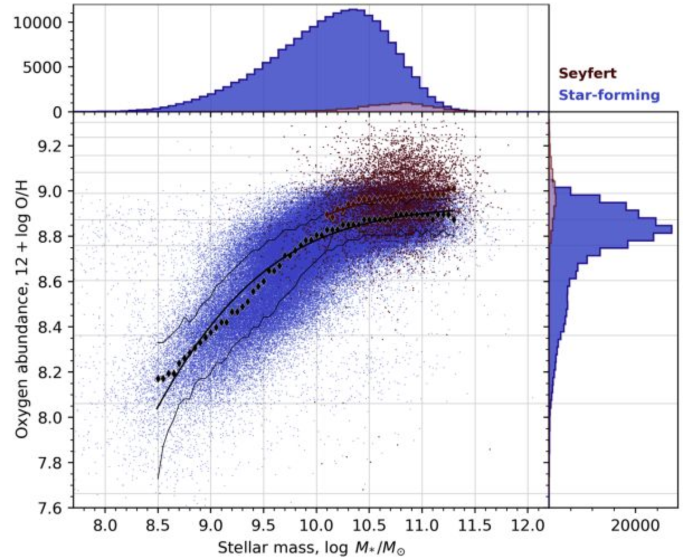

Thomas et al.
2019ApJ...874..100T

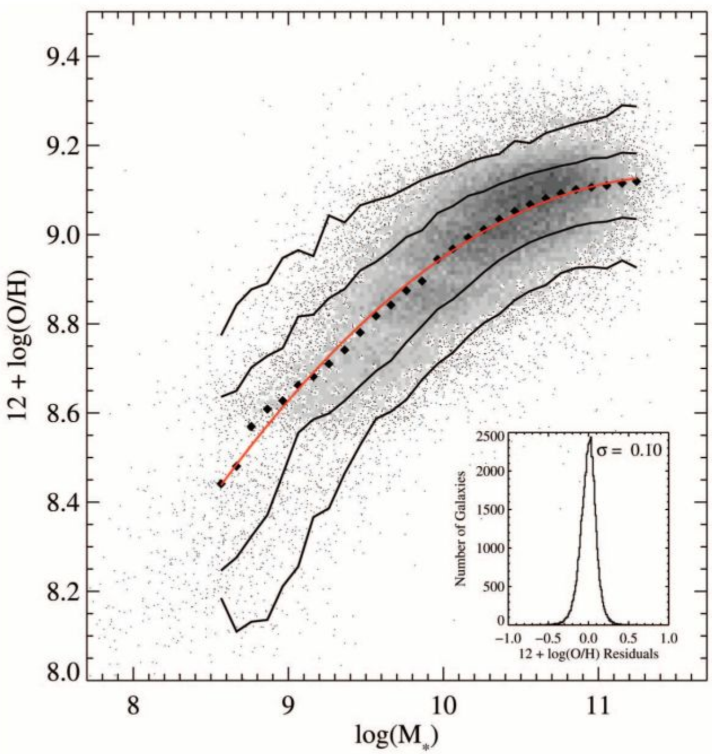

Tremonti et al. 2004ApJ...613..898T

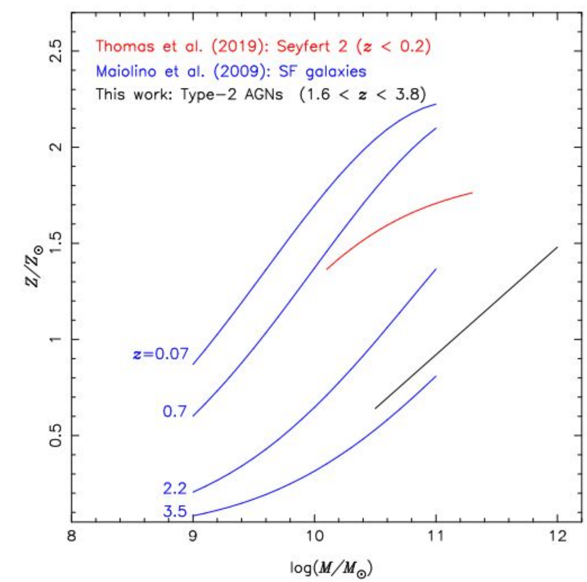

Dors et al. 2019MNRAS.486.5853D

AGN Evolution

- We know that supermassive black holes reside at the centers of almost all present-day galaxies
- Their presence has been detected through their gravitational influence on neighboring stars and gas, which orbit the holes
- We also know from local observations that a tight relation exists between
    - the mass of the black hole & the spread of stellar velocities within the host galaxy
    - or, the mass of the BH & the mass of the host galaxy
- Hints at a deep connection between the processes that formed the stars in the host and the processes that formed the central BH.

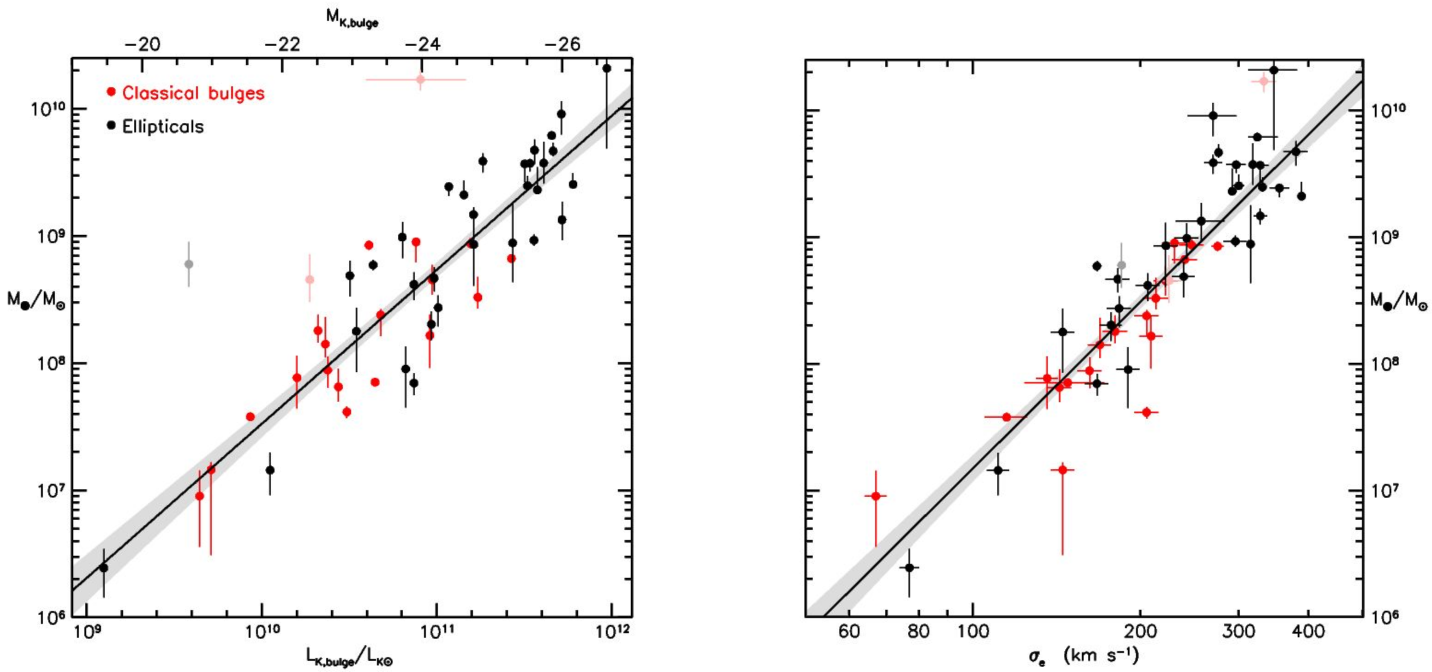

Kormendy & Ho 2013ARA1&A..51..511K

Impact of SMBH on SF

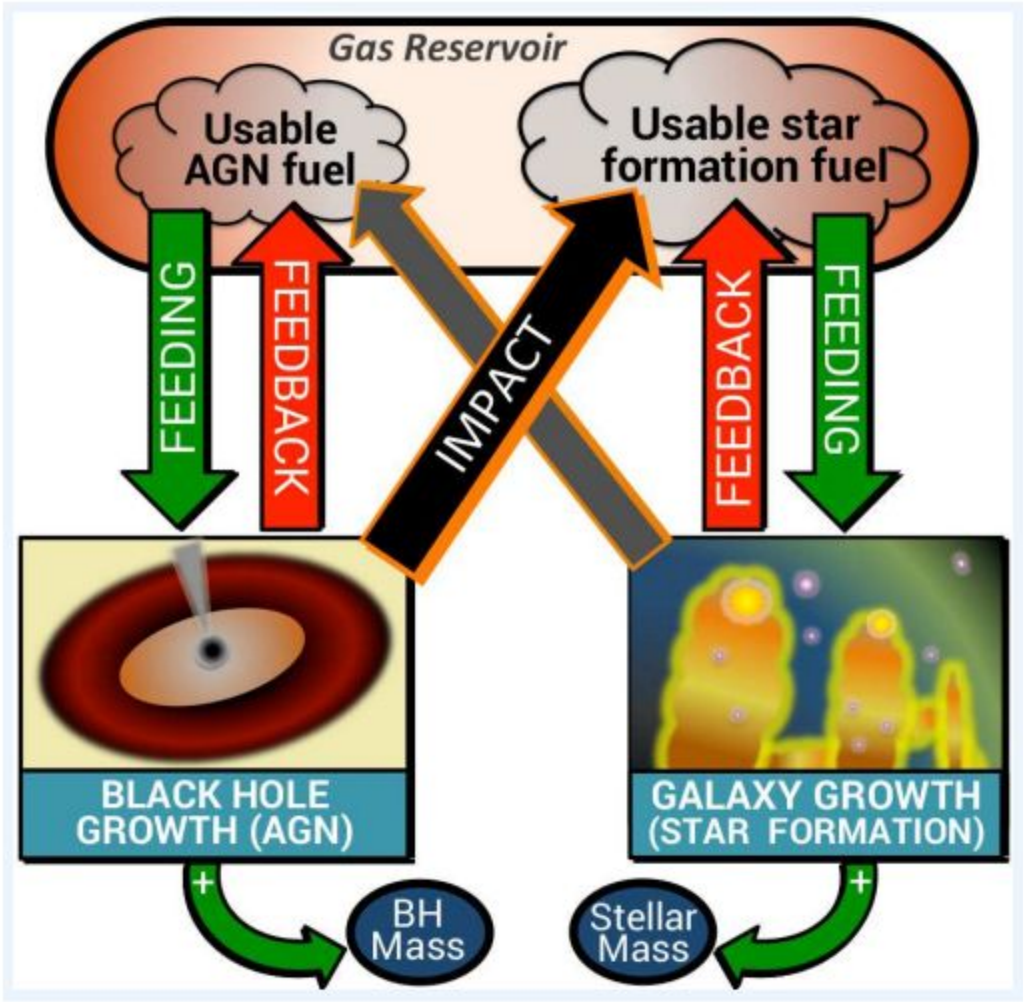

Harrison 2017NatAs...1E.165H

BAT AGN Spectroscopic Survey DR2

Hard X-rays

- directly probe AGN activity (high penetration ability)
- direct hard X-ray emission (>10 keV)
- uncontaminated by SF processes ($L_{>10\ keV}>10^{42}$ ergs s^{-1} can be considered as an AGN)
- detect all but most absorbed sources to Compton-thick levels (may miss sources with $N_H>10^{24}$ cm^{-2})
- many of the X-ray identified AGNs could not have been picked out with optical spectra alone
- Newly discovered moderate luminosity X-ray sources peak at lower z, and there are many more of them
- are there additional high-obscured sources that are missing in the 2-8 keV sample?

Swift-BAT hard X-ray all-sky survey

- All sky survey :
  - 50% of the sky each day
- wide FoV: 70° x 100°

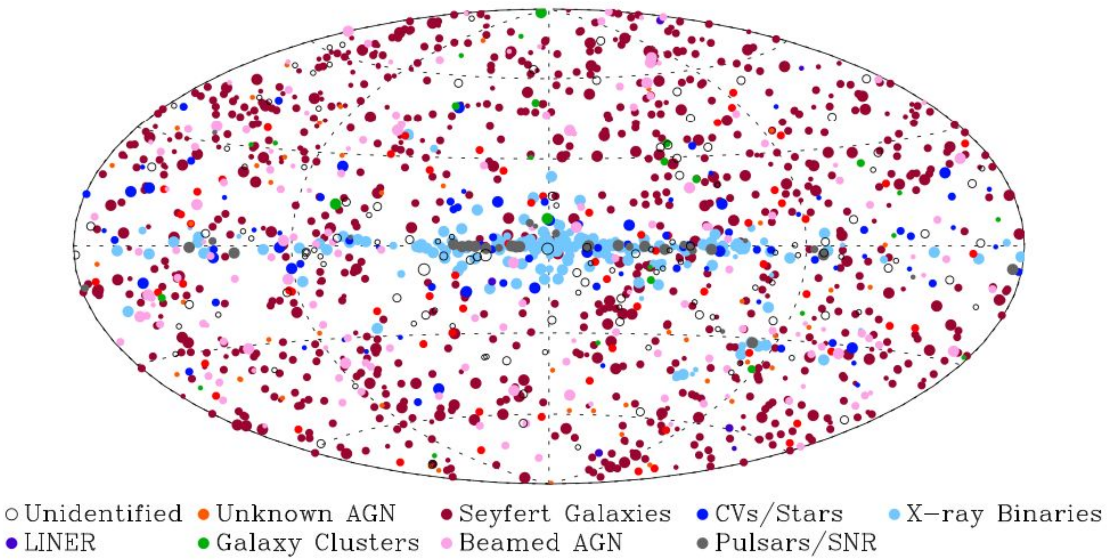

Oh et al. 2018ApJS..235....4O

BAT AGN Spectroscopic Survey DR2

Swift/BAT relatively unbiased all-sky survey of unobscured and obscured nearby AGNs up to Compton-thick levels

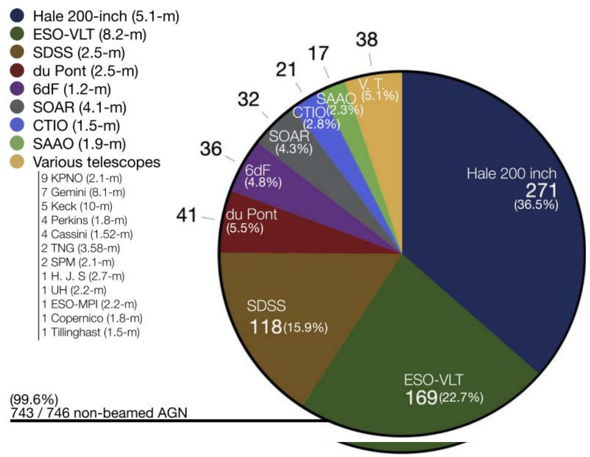

Oh et al. 2022ApJS..261....4O

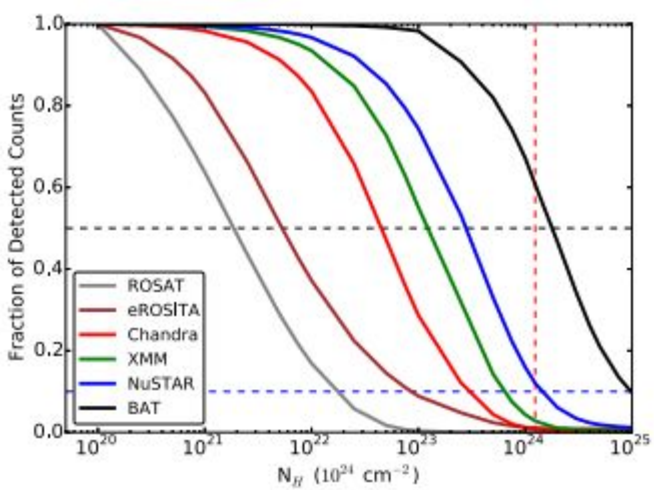

Koss et al. 2016ApJ...825...85K

BAT AGN Spectroscopic Survey

- A total of 1632 sources, of which 1105 are AGNs.

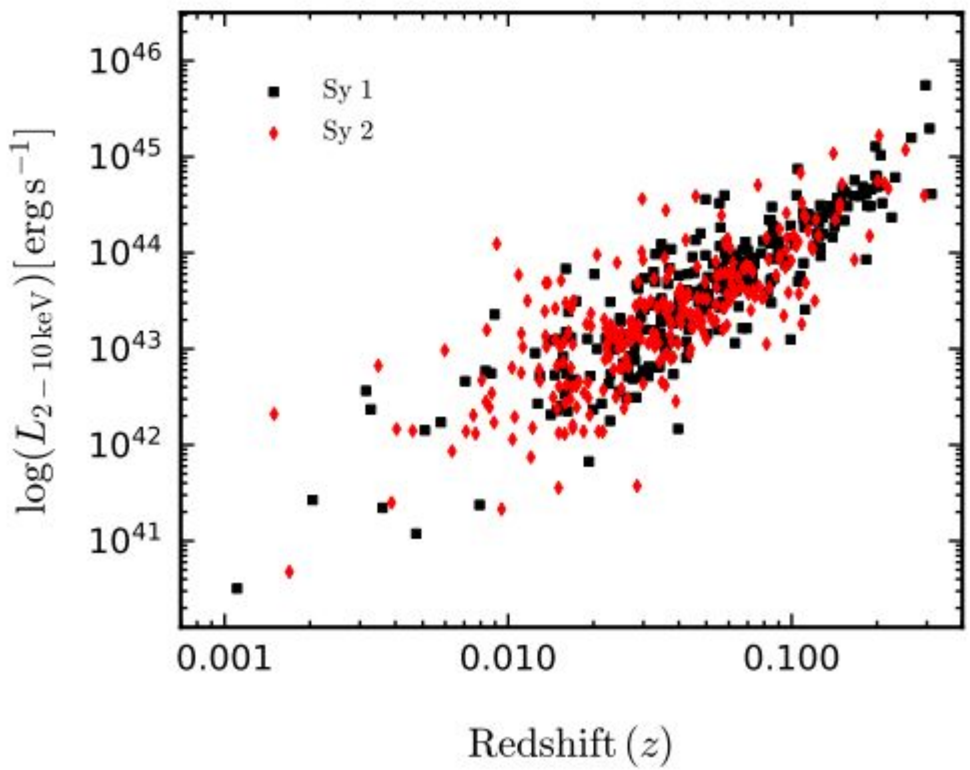

X-ray luminosity (hard; 2-8 keV and ultra-hard ≳10 keV): ANG dominant source (Lx > 10^{42} erg s^{-1}).

Selected sample

- 561 AGNs comprising of 287 Sy 1s and 274 Sy 2
    - At median redshift of z~0.04

Baldwin J. A., Phillips M. M., Terlevich R., 1981, PASP, 93, 51

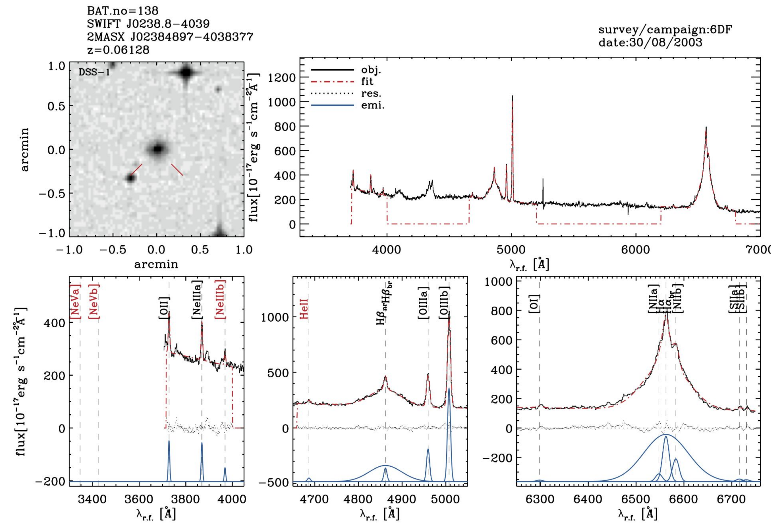

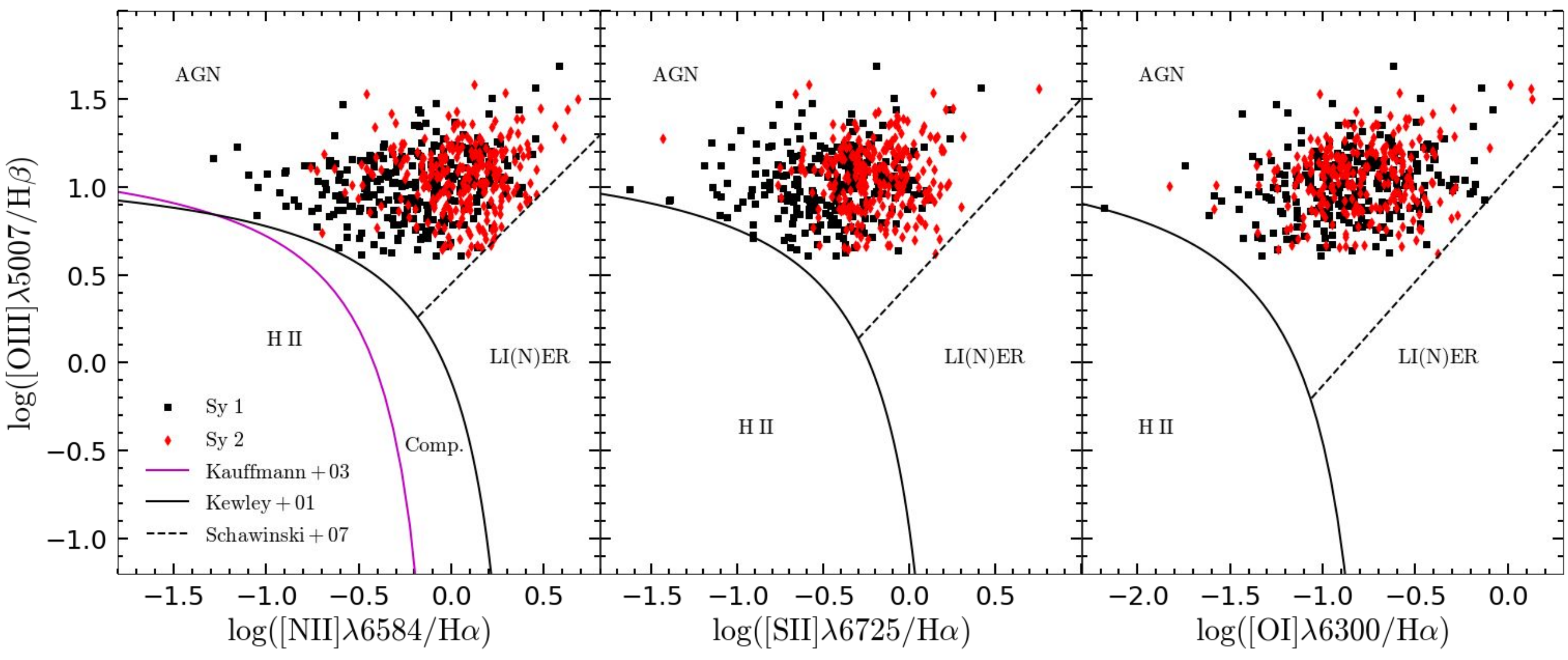

BPT diagnostics diagram

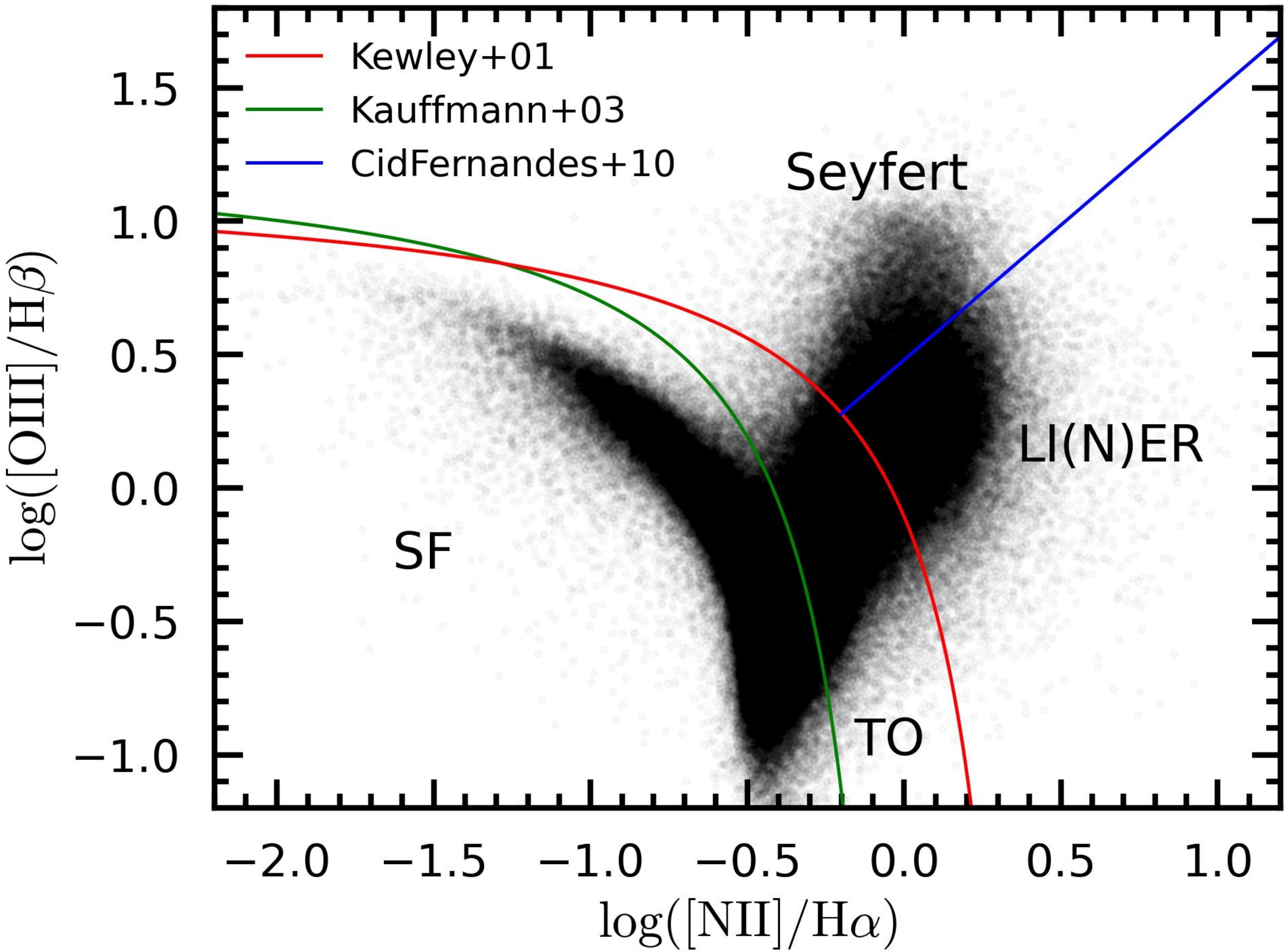

Electron temperature & density diagnostics

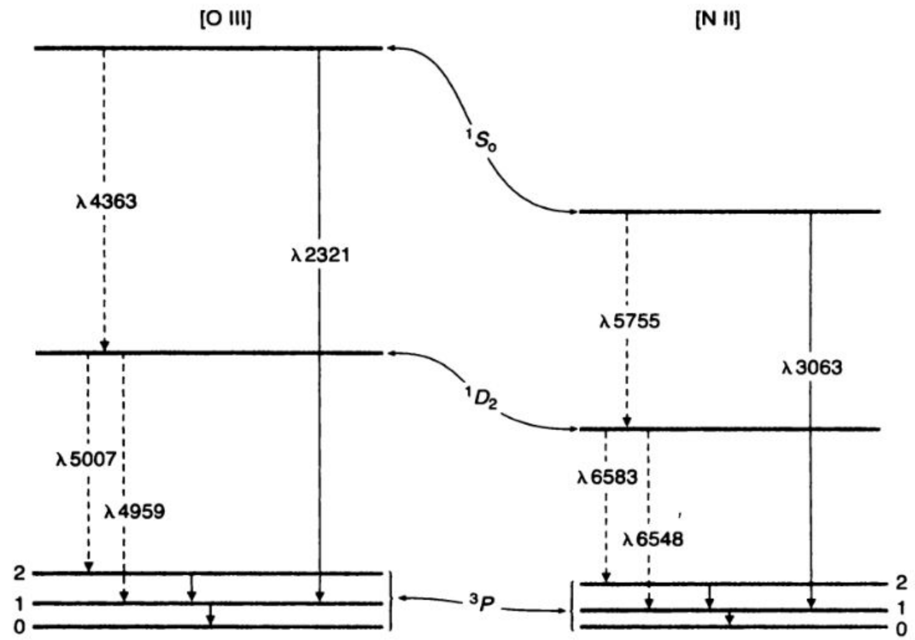

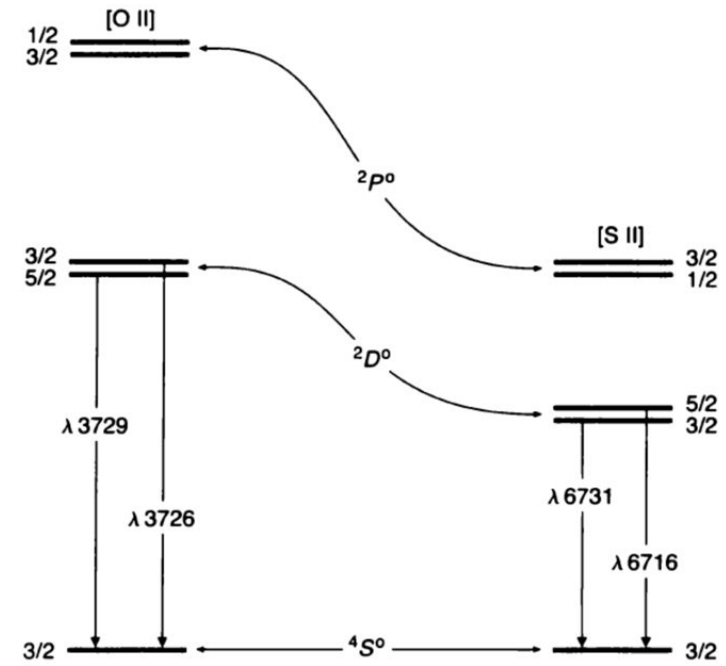

$$[\text{O III}]\frac{j_{\lambda 4959}+j_{\lambda 5007}}{j_{\lambda 4363}}=\frac{\Omega_{(^3P,^1D)}}{\Omega_{(^3P,^1S)}}\left[\frac{A_{(^1S,^1D)}+A_{(^1S,^3P)}}{A_{(^1S,^1D)}}\right]\frac{\overline{\nu}_{(^3P,^1D)}}{\nu_{4363}}\exp\left(\frac{E_{ij}}{kT_e}\right)$$

$$^1D_2 \rightarrow\ ^3P_1\ (2.513 \rightarrow 0.014\,\text{eV})$$

$$^1D_2 \rightarrow\ ^3P_2\ (2.513 \rightarrow 0.038\,\text{eV})$$

$$^1S_0 \rightarrow\ ^1D_2\ (5.354 \rightarrow 2.513\,\text{eV})$$

$$T_e = \frac{3.29\times 10^4}{\ln\left(\frac{R_{O3}}{7.90}\right)}$$

$$N_e = 10^4 \times T_e^{1/2} \times \left(\frac{R_{[\text{S II}]}-1.49}{5.62-12.8\times R_{[\text{S II}]}}\right)$$

$$R_{[\text{S II}]} = [S\ II]\frac{\lambda 6716\,\text{Å}}{\lambda 6731\,\text{Å}}$$

$$R_{O3} = [\text{O III}]\left(\frac{\lambda 4959\,\text{Å}+\lambda 5007\,\text{Å}}{\lambda 4363\,\text{Å}}\right) = [\text{O III}]\left(\frac{(4/3\times\lambda 5007\,\text{Å})}{\lambda 4363\,\text{Å}}\right)$$

Osterbrock & Ferland1, 20061

T_e-method

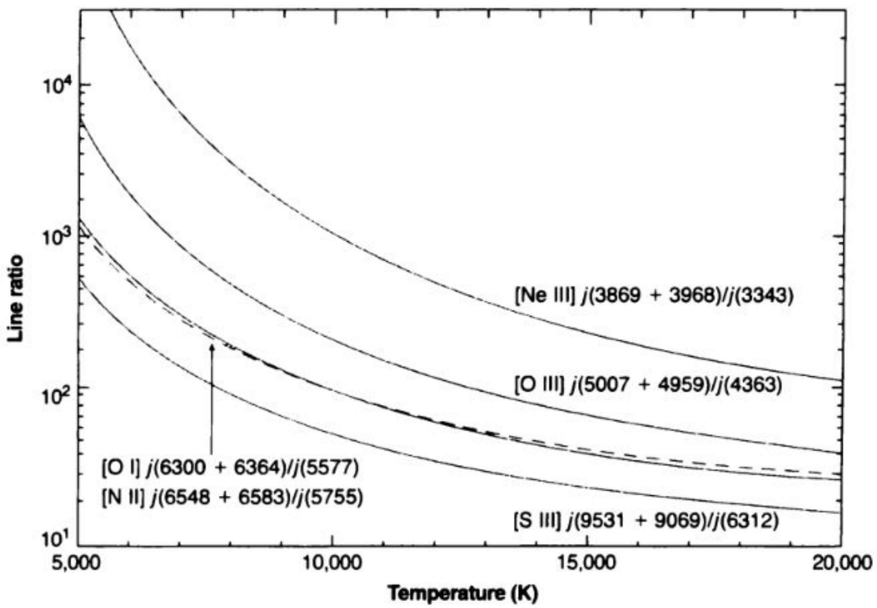

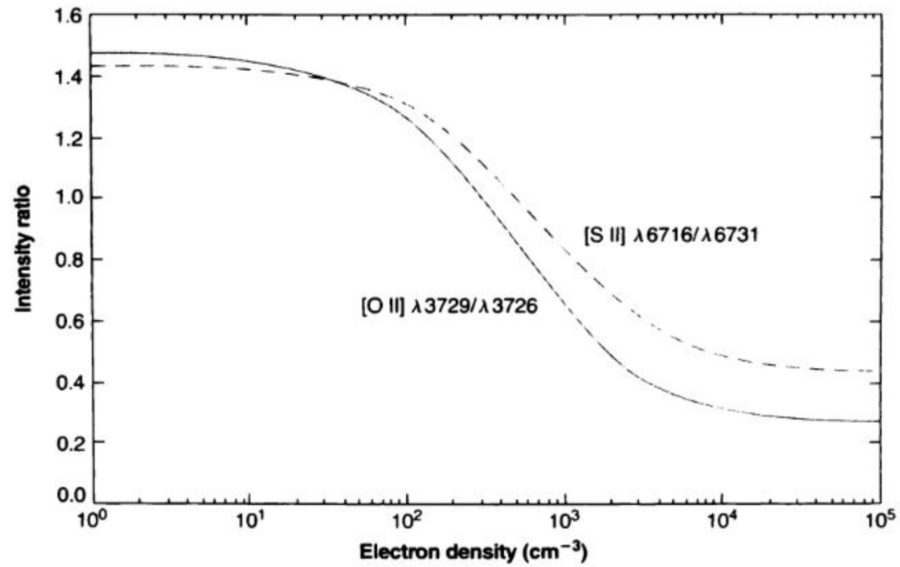

Osterbrock & Ferland1, 20061

$$t_3 = 0.8254 - 0.0002415 \times R_{O3} + \frac{47.77}{R_{O3}}$$

$$t_2 = (\mathrm{a} \times t_3^3) + (\mathrm{b} \times t_3^2) + (\mathrm{c} \times t_3) + \mathrm{d}$$

$$\mathrm{a} = 0.17,\ \mathrm{b} = -1.07,\ \mathrm{c} = 2.07 \text{ and } \mathrm{d} = -0.33$$

$$12 + \log\left(\frac{\mathrm{O}^{2+}}{\mathrm{H}^+}\right) = \log\left(\frac{I(4959\,\text{Å}) + I(5007\,\text{Å})}{I(\mathrm{H}\beta)}\right) + 6.144 + \frac{1.251}{t_3} - 0.55 \times \log t_3$$

$$12 + \log\left(\frac{\mathrm{O}^{+}}{\mathrm{H}^+}\right) = \log\left(\frac{I(3727\,\text{Å})}{I(\mathrm{H}\beta)}\right) + 5.992 + \frac{1.583}{t_2} - 0.681 \times \log t_2 + \log[1 + 2.3 n_e]$$

$$\mathrm{N}\left(\frac{\mathrm{O}}{\mathrm{H}}\right) = \mathrm{ICF(O)} \times \mathrm{N}\left(\frac{\mathrm{O}^{2+}}{\mathrm{H}^+} + \frac{\mathrm{O}^{+}}{\mathrm{H}^+}\right)$$

$$\mathrm{ICF(O)} = \frac{N(\mathrm{He}^+) + N(\mathrm{He}^{2+})}{N(\mathrm{He}^+)}$$

Peimbert & Castro 969BOTT....5....3P

Strong Line Method

- Storchi-Bergmann et al. (1998, hereafter SB98f1)
  - Requires electron density correction

$$12 + (O/H) = 8.34 + (0.212\,x) - (0.012\,x^2) - (0.002\,y) + (0.007\,xy) - (0.002\,x^2 y) + (6.52 \times 10^{-4}\,y^2) + (2.27 \times 10^{-4}\,xy^2) + (8.87 \times 10^{-5}\,x^2 y^2),$$

x = [N II]$\lambda\lambda$6548,6584/Hα and y = [O III]$\lambda\lambda$4959,5007/Hβ.

$$\log(O/H)_{SB98f1} = [\log(O/H)] - \left[0.1 \times \log \frac{N_e(\mathrm{cm}^{-3})}{300\ (\mathrm{cm}^{-3})}\right]$$

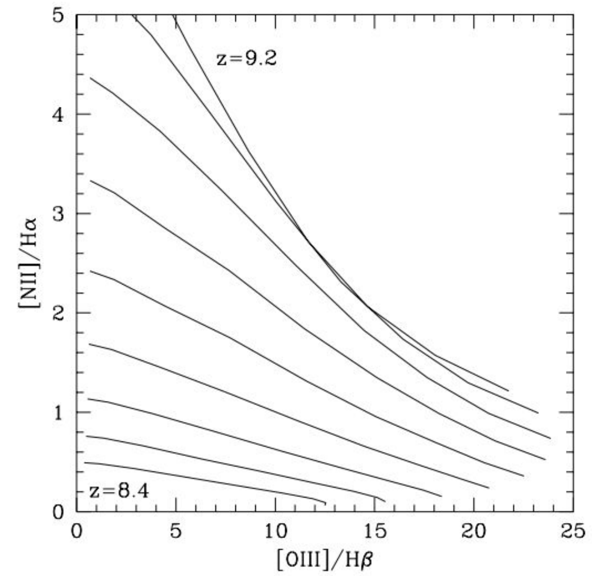

- Carvalho et al. (2020, hereafter C20)
  - No electron density correction

$$(Z_{NLR}/Z_{\odot}) = (4.01 \pm 0.08)^{N2} - 0.07 \pm 0.01$$

$$N2 = \log([\mathrm{N\,II}]\lambda6584/\mathrm{H}\alpha)$$

$$12 + \log(O/H)_{C20} = 12 + \log[(Z_{NLR}/Z_{\odot}) \times 10^{\log(O/H)_{\odot}}]$$

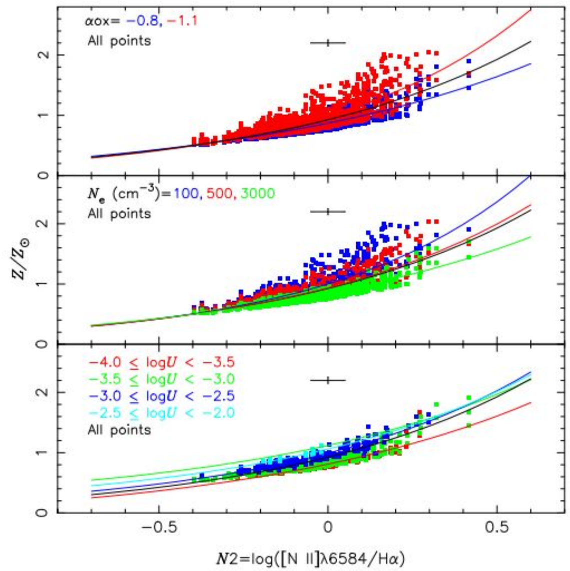

Is there evidence for [O III] variability in Seyferts?

- The results are contradictory
  - Apparent [O III] variability in the narrow line Seyfert I Mrk 142 (Zhang et al. 2016MNRAS.457L..64Z)
  - No evidence for [O III] variability in Mrk 142 (Barth et al. 2016MNRAS.458L.109B)

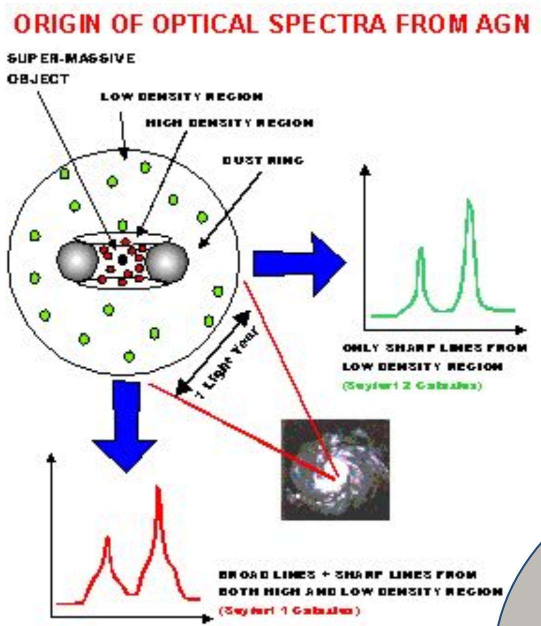

Different orientation of the source with respect to the observer. In type 2 Seyfert galaxies a dust ring hide the high density core and thus the broad permitted lines are no more visible.

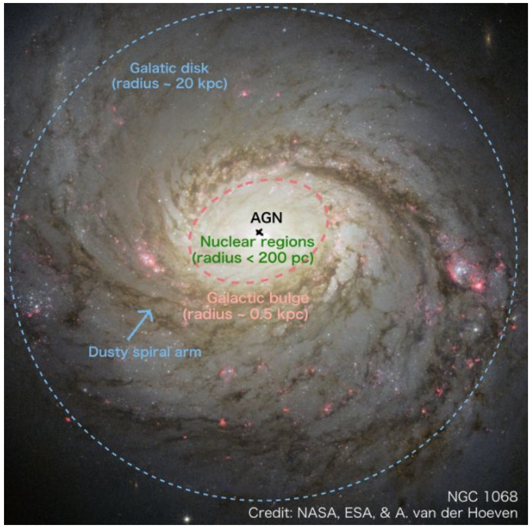

A compact core component and an extended component, observed on both sides of the nucleus and extending from 14 kpc southeast to 12 kpc northwest in the NLS1 by Congiu et al. 2017, A&A, 603, A32.

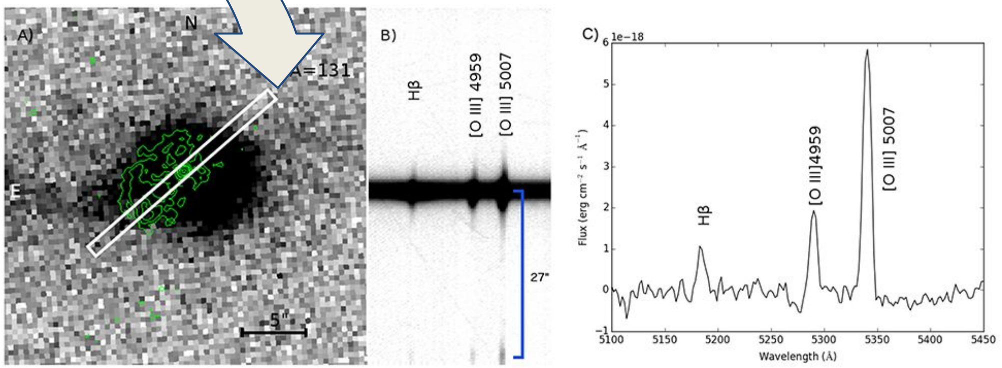

What are the real densities in the NLRs?

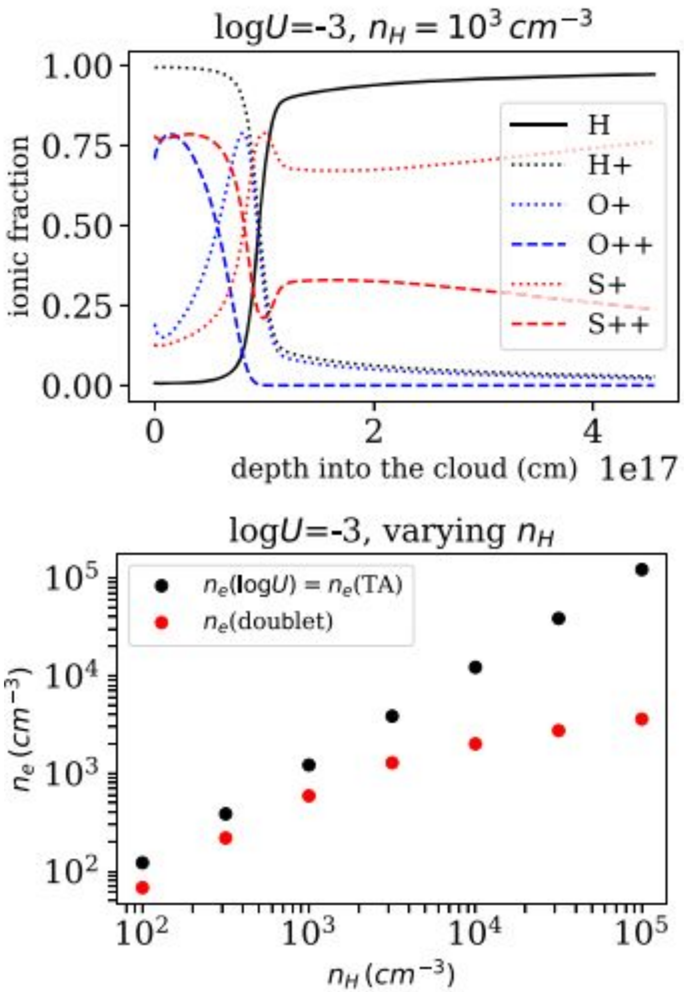

Davies et al. 2020MNRAS.498.4150D

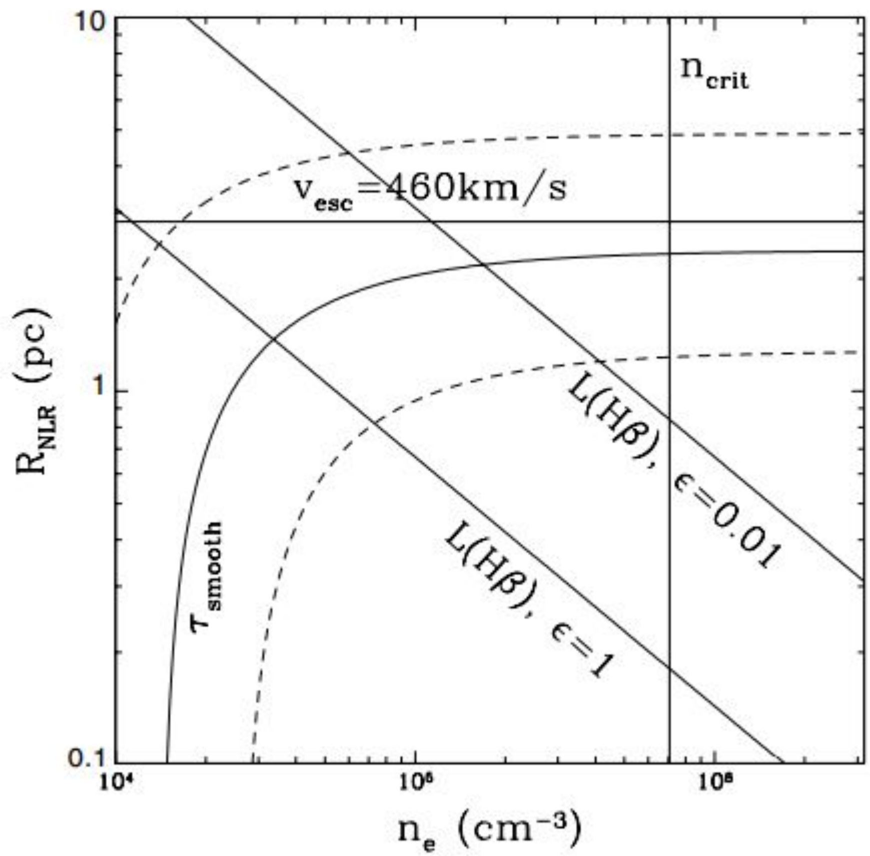

Peterson et al. 2013ApJ...779..109P

How Electron Density Affect Metallicities?

- Density values lower than the critical density have insignificant effects on the emission line ratios used for the metallicity estimations

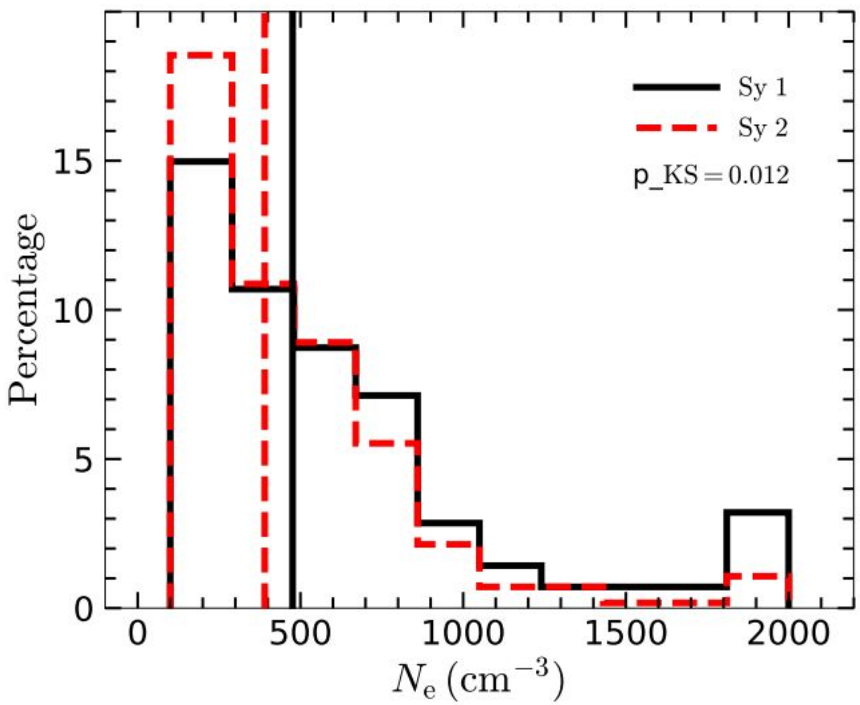

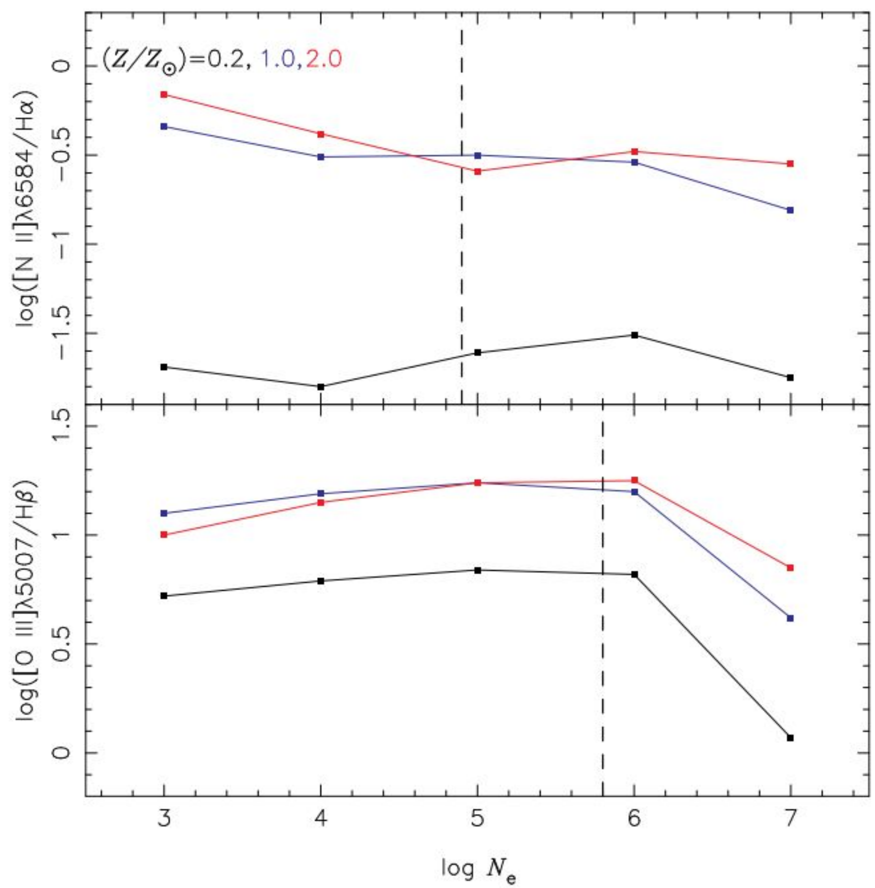

Gas-phase metallicity

- Oxygen abundances relative to hydrogen (O/H) in the narrow line region (NLR) gas phases of Seyfert 1 (Sy 1) and Seyfert 2 (Sy 2).
- Sy 1 have 0.2 dex (mean) lower abundances than Sy 2, but these differences do not have a statistically significant difference (from KS-test).

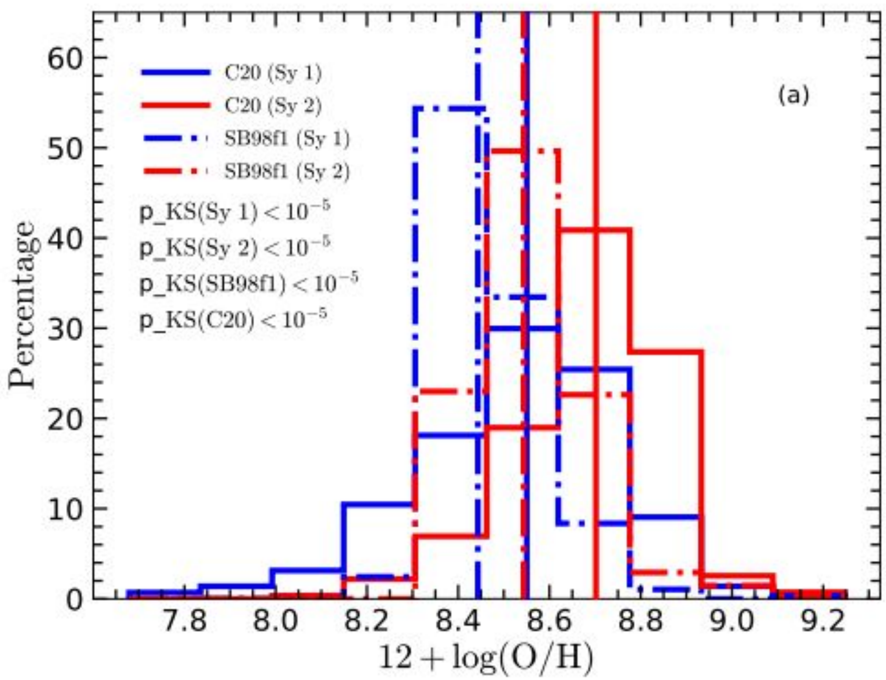

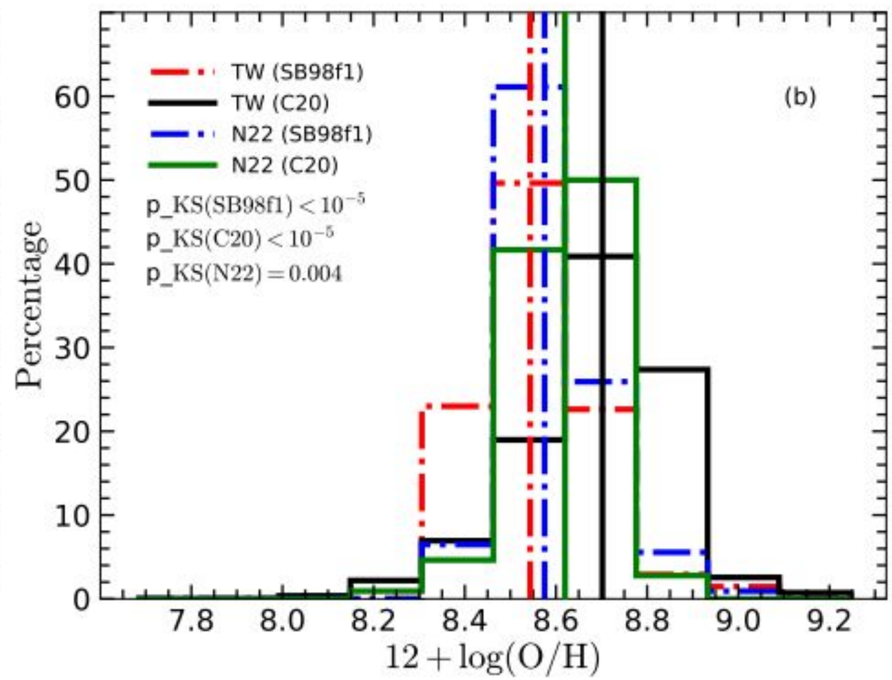

Metallicity-luminosity relation

- The metallicities decrease with increasing X-ray luminosities

$$\log[L_{\rm bol}({\rm erg\,s^{-1}})] = (0.0378 \times \log L_{\rm X}^2) - (2.00 \times \log L_{\rm X}) + 60.5$$

$$\log[L_{\rm bol}({\rm erg\,s^{-1}})] = (0.0378 \times \log L_{\rm X}^2) - (2.03 \times \log L_{\rm X}) + 61.6$$

$$L_{\rm X}({\rm erg\,s^{-1}}) = L_{2-10}^{\rm obs} \text{ and } L_{14-195}^{\rm obs}$$

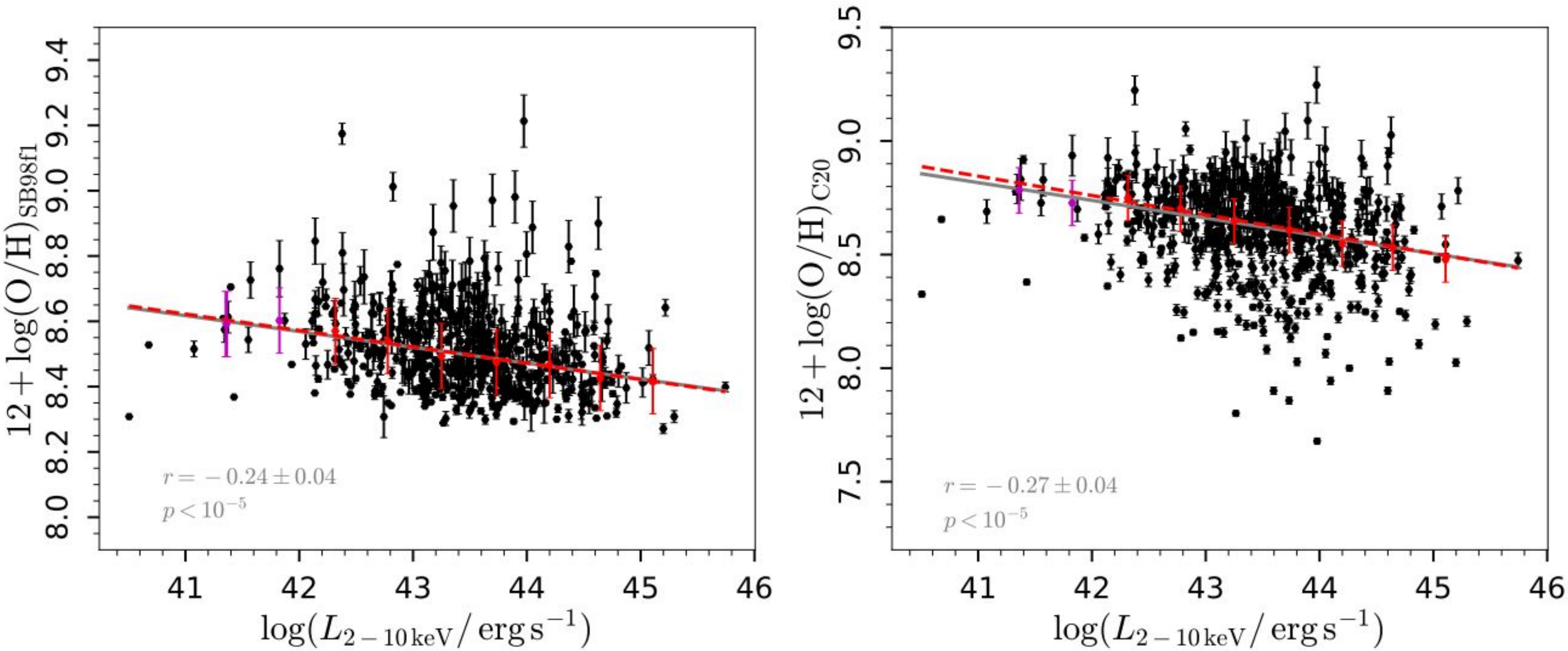

The Mass-Metallicity Relation

- MZR follow a downward redshift evolution (from lower to higher redshifts), similar to that of SF galaxies.

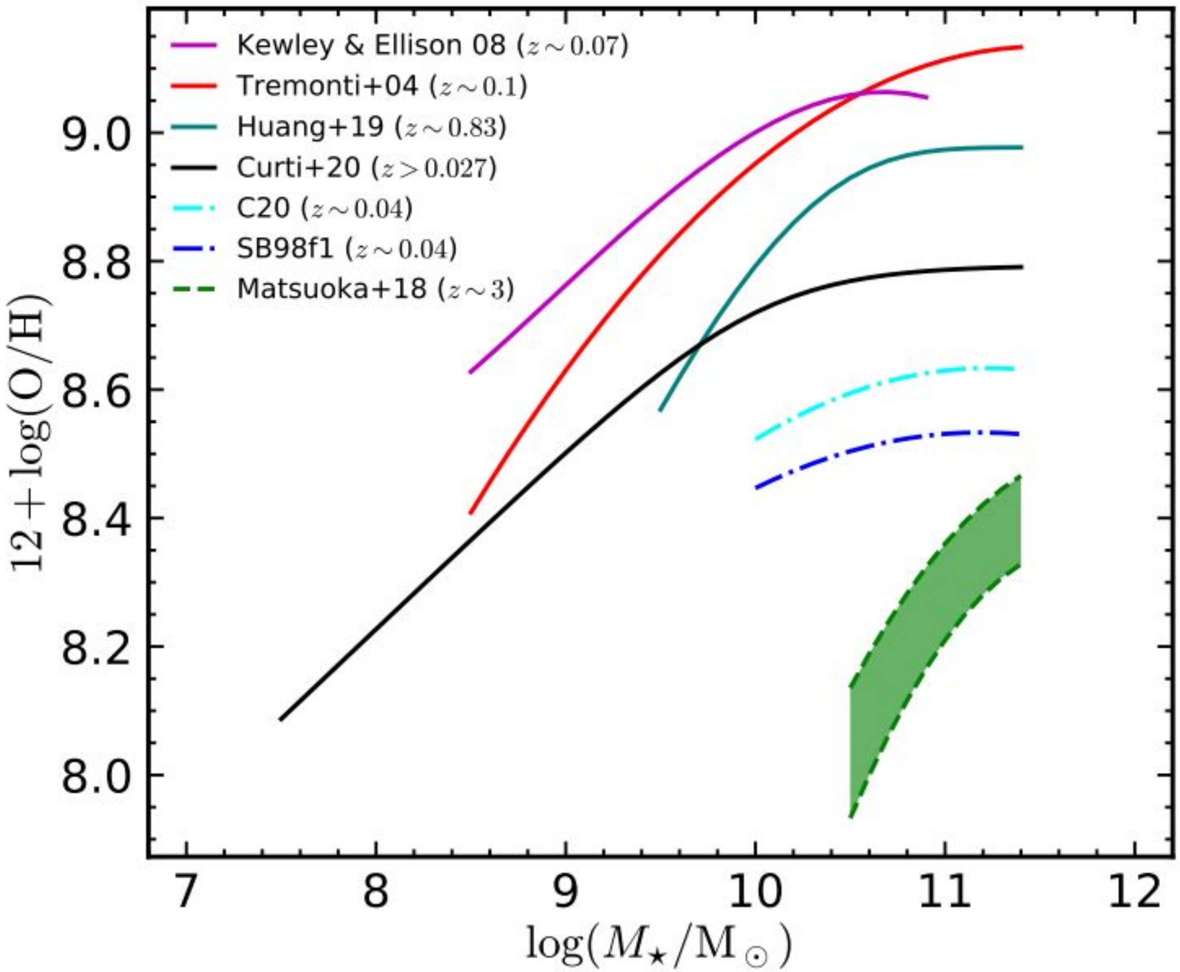

$$12 + \log(\mathrm{O/H}) = Z_0 - \frac{\gamma}{\beta} \log\left(1 + \left(\frac{M}{M_0}\right)^{-\beta}\right)$$

AGN intrinsic properties

- The supermassive black hole mass and accretion rate

$$\log[L_{\rm bol}({\rm erg\,s^{-1}})] = (0.0378 \times \log L_{\rm X}^2) - (2.00 \times \log L_{\rm X}) + 60.5$$

$$\log[L_{\rm bol}({\rm erg\,s^{-1}})] = (0.0378 \times \log L_{\rm X}^2) - (2.03 \times \log L_{\rm X}) + 61.6$$

$$L_{\rm X}({\rm erg\,s^{-1}}) = L_{2-10}^{\rm obs} \text{ and } L_{14-195}^{\rm obs}$$

$$\log\left(\frac{M_{\rm BH}}{M_\odot}\right) = a \times \log\left(\frac{\sigma_*}{200\,{\rm km\,s^{-1}}}\right) + b$$

where $a = 8.14 \pm 0.20$ is the slope and $b = 3.38 \pm 0.65$ is the zero point.

$$L_{\rm Edd} = 1.3 \times 10^{46}\,{\rm erg\,s^{-1}}\,\frac{M_{\rm BH}}{10^8 M_\odot}$$

Metallicity and accretion rate

- The effect of decreasing metallicity with increasing X-ray luminosity leading to significant correlation between metallicity and accretion rate.

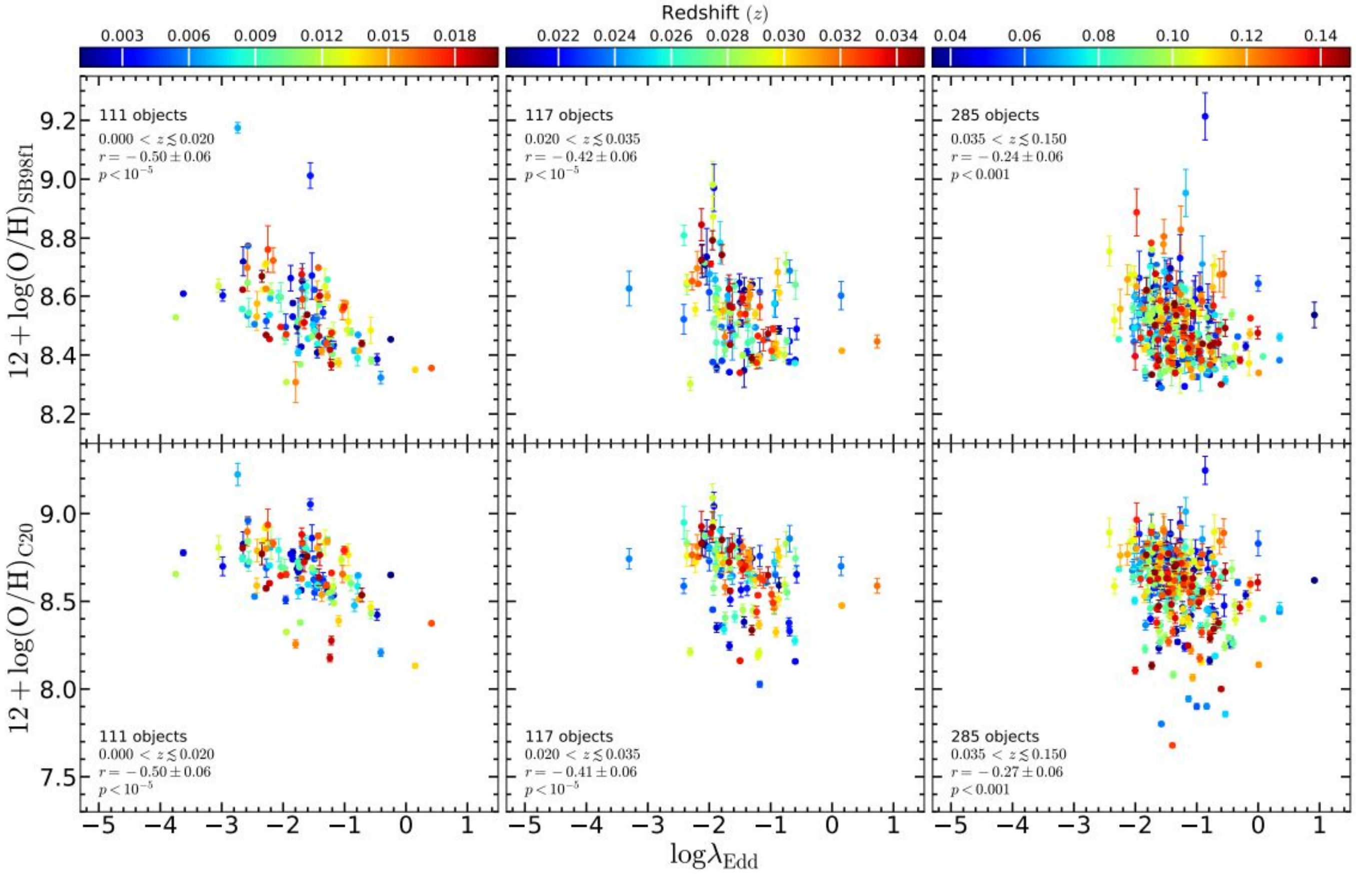

Conclusion

Summary of the Key findings are summarized below:

- Comparison of the NLRs O/H between Sy 1s and Sy 2s show statistically insignificant disparity.
- AGN metallicities are related to the hosts stellar masses following a downward redshift evolution, similar to that of SF galaxies, from lower to higher redshifts.
- Comparison of O/H with the literature indicates lower values (a mean difference of 0.2-0.5 dex) in AGN hosts than in SF galaxies.
- The metallicities decrease with increasing X-ray luminosities and have significant correlations with accretion rates at the redshift range $z \lesssim 0.02$.
- AGNs are driving the chemical enrichment of their host galaxies, as a result of the inflow of pristine gases that are diluting the more metal-rich gases, together with a recent cessations on the star formation.

Monthly Notices of the ROYAL ASTRONOMICAL SOCIETY

MNRAS **520,** 1687–1703 (2023)
Advance Access publication 2023 January 20

https://doi.org/10.1093/mnras/stad217

Oxygen abundances in the narrow line regions of Seyfert galaxies and the metallicity–luminosity relation

Mark Armah,[1★] Rogério Riffel,[1,2★] O. L. Dors,[3] Kyuseok Oh,[4,5] Michael J. Koss,[6,7] Claudio Ricci,[8,9] Benny Trakhtenbrot,[10] Mabel Valerdi,[11] Rogemar A. Riffel[2,12] and Angela C. Krabbe[3]

[1]*Departamento de Astronomia, Instituto de Física, Universidade Federal do Rio Grande do Sul, CP 15051, 91501-970 Porto Alegre, RS, Brazil*
[2]*Laboratório Interinstitucional de e-Astronomia - LIneA, Rua General José Cristino 77, Rio de Janeiro, RJ - 20921-400, Brazil*
[3]*Universidade do Vale do Paraíba. Av. Shishima Hifumi, 2911, CEP: 12244-000, São José dos Campos, SP, Brazil*
[4]*Korea Astronomy and Space Science Institute, Daedeokdae-ro 776, Yuseong-gu, Daejeon 34055, Republic of Korea*
[5]*Department of Astronomy, Kyoto University, Kitashirakawa-Oiwake-cho, Sakyo-ku, Kyoto 606-8502, Japan*
[6]*Eureka Scientific, 2452 Delmer Street Suite 100, Oakland, CA 94602-3017, USA*
[7]*Space Science Institute, 4750 Walnut Street, Suite 205, Boulder, Colorado 80301, USA*
[8]*Núcleo de Astronomía de la Facultad de Ingeniería, Universidad Diego Portales, Av. Ejército Libertador 441, Santiago 22, Chile*
[9]*Kavli Institute for Astronomy and Astrophysics, Peking University, Beijing 100871, People's Republic of China*
[10]*School of Physics and Astronomy, Tel Aviv University, Tel Aviv 69978, Israel*
[11]*Instituto Nacional de Astrofísica, Óptica y Electrónica (INAOE), Luis E. Erro No. 1, Sta. Ma. Tonantzintla, Puebla, C.P. 72840, México*
[12]*Departamento de Física, CCNE, Universidade Federal de Santa Maria, 97105-900 Santa Maria, RS, Brazil*

Integral field spectroscopy

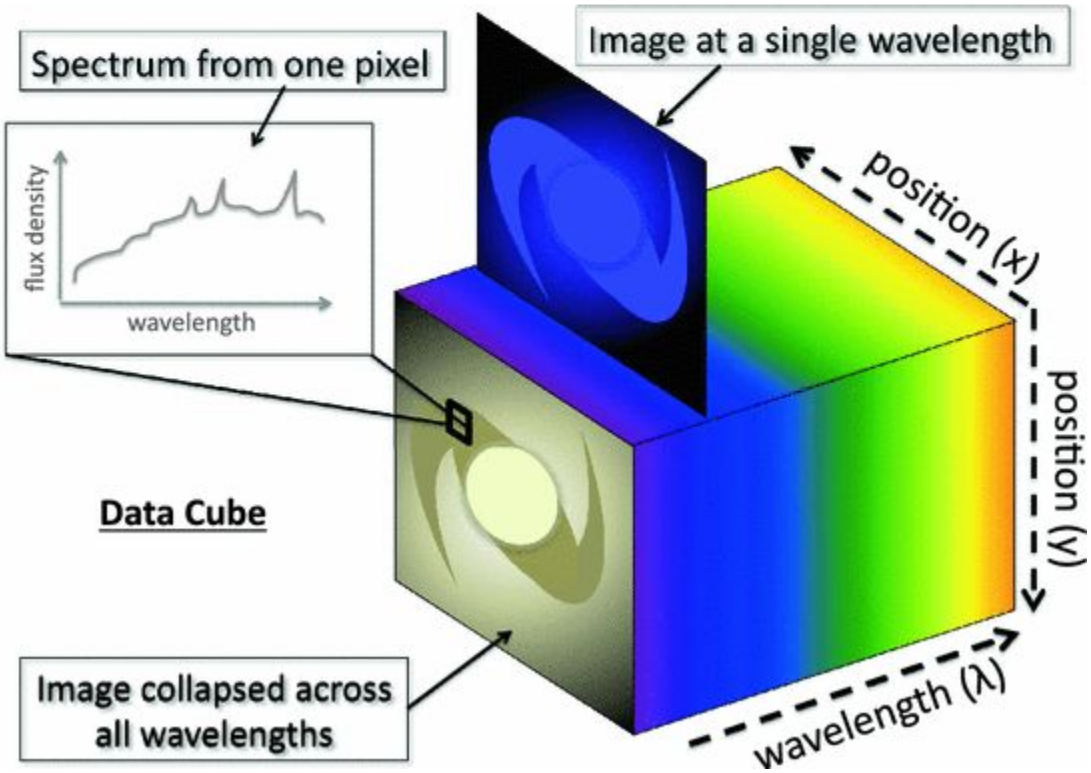

- Gemini Multi-Object Spectrographs (GMOS)
- Multi Unit Spectroscopic Explorer (MUSE)

Spatially-resolved metallicities in Seyfert galaxies

$$E(B-V) = \frac{E(H\beta - H\alpha)}{k(H\beta) - k(H\alpha)} = \frac{2.5}{k(H\beta) - k(H\alpha)} \left[\frac{(F_{H\alpha}/F_{H\beta})^{obs}}{(F_{H\alpha}/F_{H\beta})^{int}} \right]$$

$$c(H\beta) = -\frac{1}{f(\lambda) - f(H\beta)} \cdot \left[\log\left(\frac{F(\lambda)}{F(H\beta)}\right) - \log\left(\frac{I(\lambda)}{I(H\beta)}\right) \right]$$

$$A_V = 3.1 \cdot E(B-V) = 2.15 c(H\beta)$$

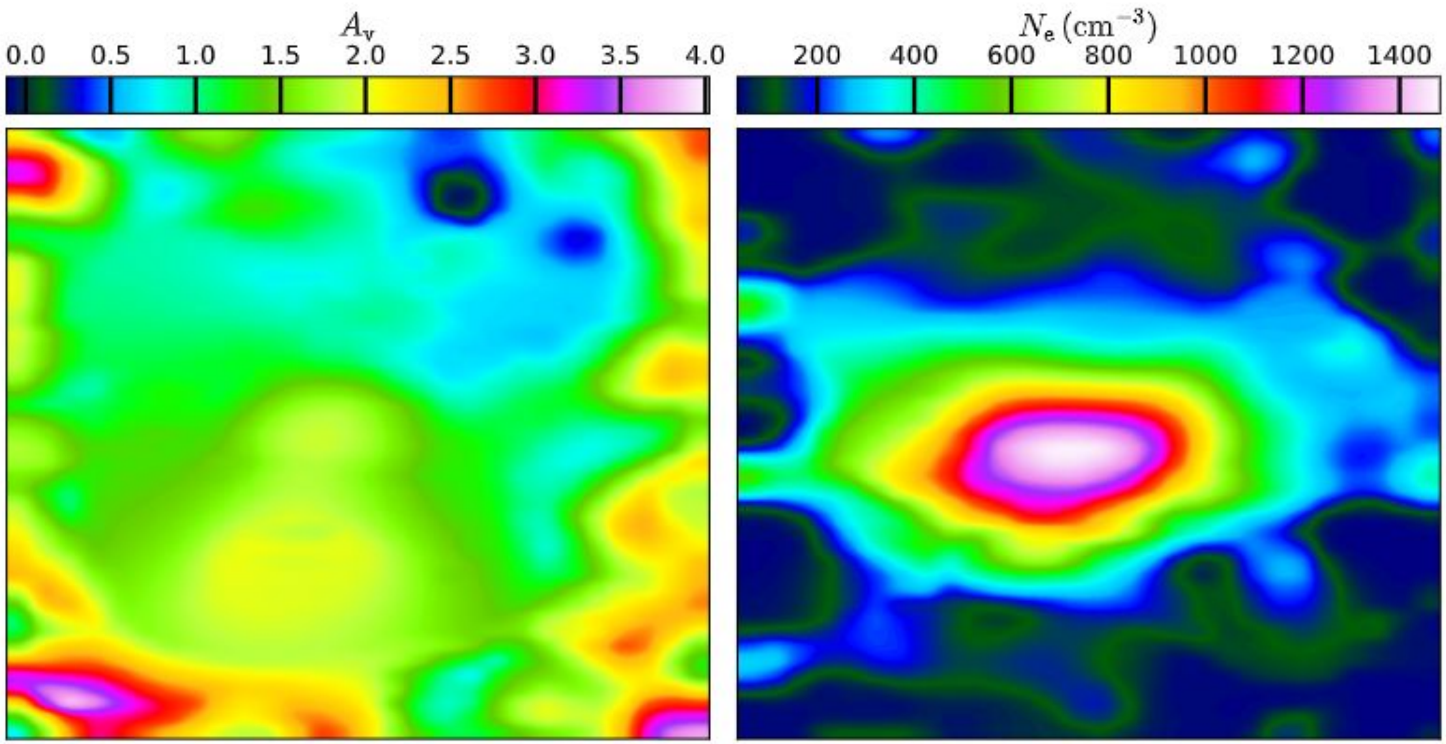

$$\frac{I_\lambda}{I(H\beta)} = \frac{I_{\lambda,0}}{I(H\beta)_0} 10^{-c[f(\lambda) - f(H\beta)]} = \frac{I_{\lambda,0}}{I(H\beta)_0} 10^{-c(H\beta)\left[\frac{f(\lambda)}{f(H\beta)} - 1\right]}$$

Spatially-resolved metallicities in Seyfert galaxies

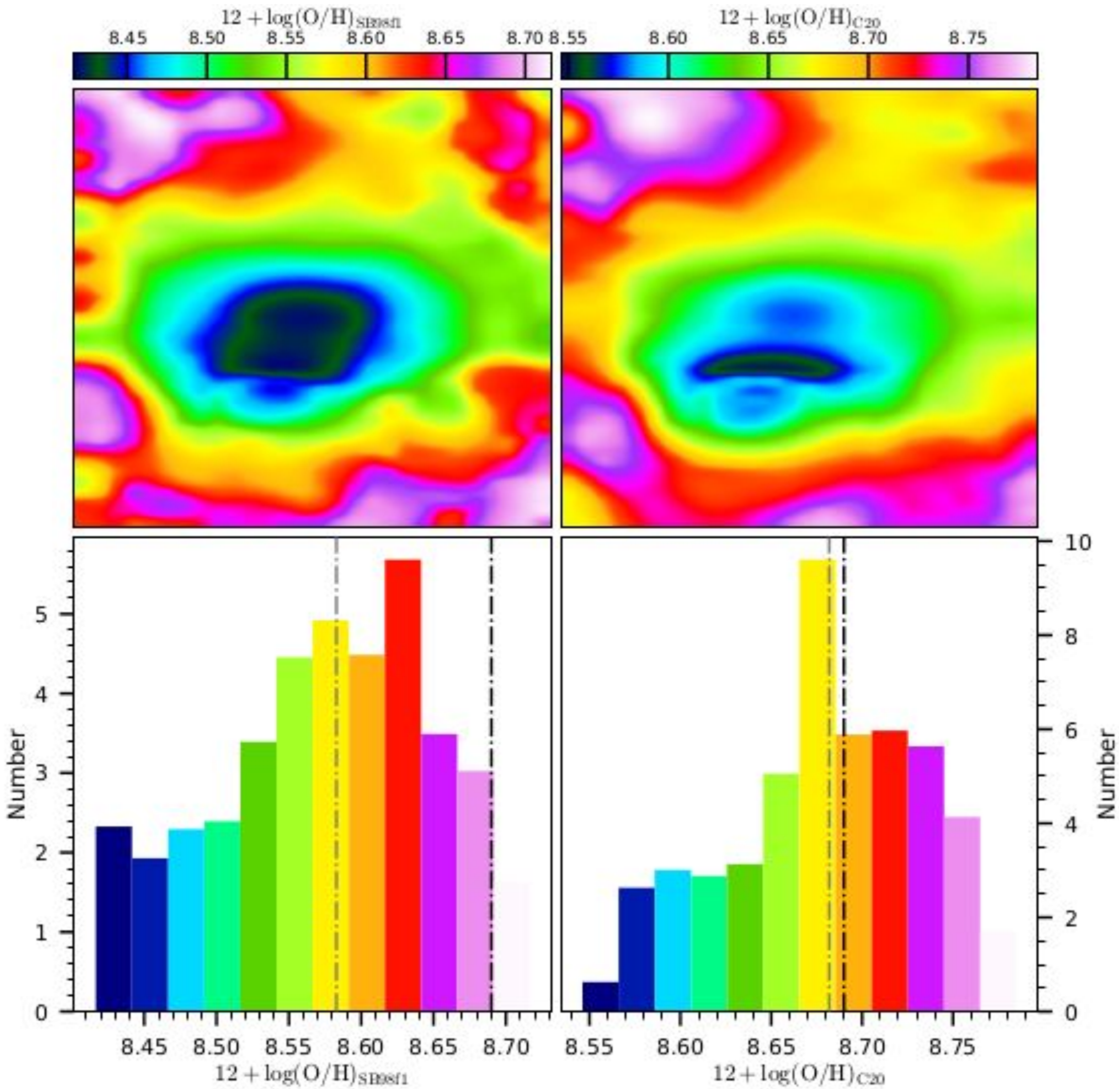

Next step

$$L_\gamma = 1.6 \times 10^{-6} \times 4\pi d_L^2 E_1 \frac{(1-\Gamma)}{(2-\Gamma)} \frac{\left[\left(\frac{E_2}{E_1}\right)^{2-\Gamma} - 1\right]}{\left[\left(\frac{E100}{E_1}\right)^{1-\Gamma} - 1\right]} \times F_{100}.$$

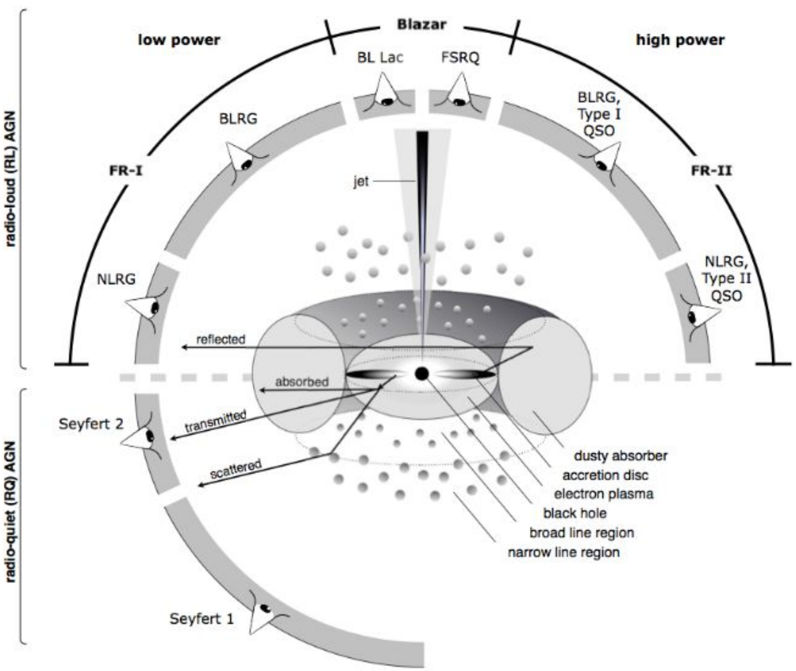

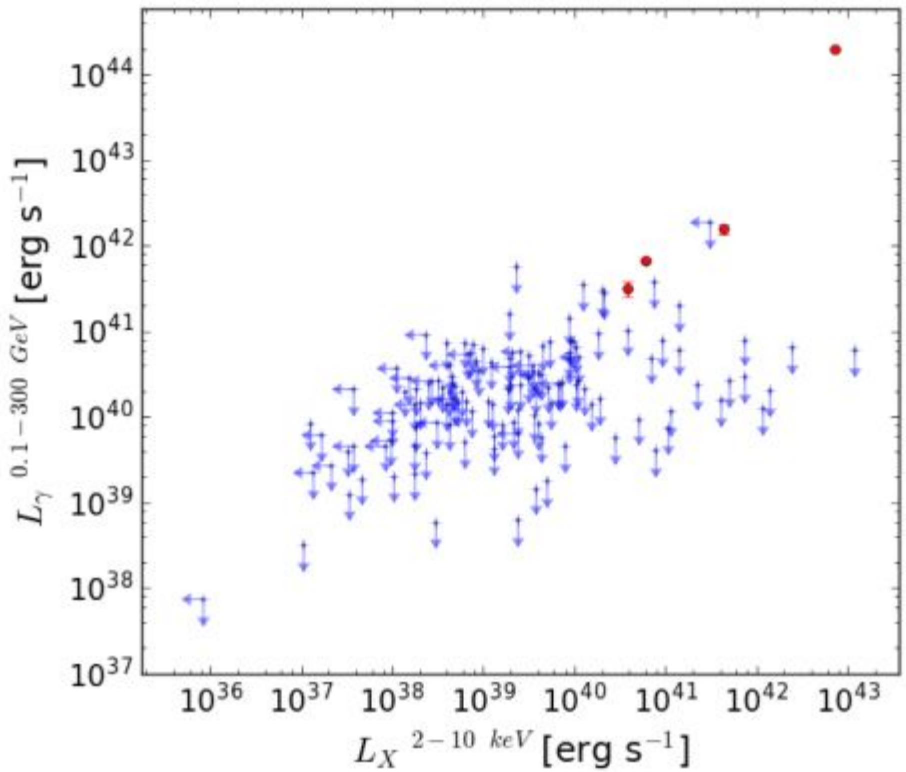

Identification issues
MRK 273
IRAS F13428+5608
A1342+56
UGC 86961
MCG+9-23-4
IZw 71
VV 851

de Menezes et al. 2020MNRAS.492.4120D

Bayesian H II-CHI-MISTRY code

“I am an astronomer who can't see the stars”

Thank You